The role of non-bonding electron pairs in intermetallic compounds

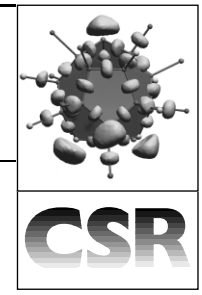

Thomas F. Fässler

Eduard-Zintl-Institute, Darmstadt Technical University, Petersenstr. 18, D-64287 Darmstadt. E-mail: faessler@ac.chemie.tu-darmstadt.de; Fax: +49-6151 166029; Tel: +49-6151 162292

Received 6th September 2002
First published as an Advance Article on the web 15th January 2003

The Electron Localisation Function, *ELF* pictorially visualises chemists' intuitive ideas of single and multiple bonds as well as non-bonding electron pairs in molecules. The power of the representation of chemical bonds *via ELF* is that on the one hand covalent, polar, and ionic bonds are distinguishable, and that on the other hand ELF can be calculated for molecules *and* solids. This enables us to transfer the ideas of chemical bonding from molecular to intermetallic compounds. Localised two-electron-two-centre bonds and lone pairs are present in solid-state valence compounds (Zintl phases) as expected by the 8-N rule. In solids, lone pairs are generally more contracted than in molecules due to 'lone-pair repulsion'. In intermetallic compounds localised electrons predominantly occur in the form of lone pairs. Lattice vibrations influence the strength of lone pair interactions and non-bonded interactions lead to an exchange of delocalised and localised electrons. Such a mechanism of local electron pair formation gives rise to ideas of a *chemical view* of the phenomenon of superconductivity in intermetallic compounds.

Thomas F. Fässler studied chemistry and mathematics at the University of Konstanz, Germany. In 1988 he received his PhD for his work on transition metal cluster compounds under the supervision of Professor G. Huttner from the University of Heidelberg, Germany. During a period of research at the University of Chicago, USA with Professor J. Burdett he carried out fundamental theoretical studies on chemical bonding at metal surfaces. From 1991 to 1999 he stayed at the ETH Zurich, Switzerland where he developed his present research fields and completed his Habilitation. The appointment to his Full Professorship at the Darmstadt Technical University, Germany, followed in 2000. Since 2001 he has been director of the Institute of Inorganic Chemistry at the Technical University Darmstadt. His research interests are focused at the interface between molecular and solid state-chemistry, and involve synthesis, structural characterisation, as well as the study of the electronic properties and chemical bonding of soluble main group element clusters (Zintl ions), fullerides, and intermetallic compounds.

1 Introduction

In strong contrast to the description of chemical bonds in molecules, the picture of chemical bonding in metals and intermetallic compounds is still in an unsatisfactory state.[1,2] Several concepts and rules help chemists to understand the stability, the reactivity, and the structure of molecular compounds. The octet rule, Lewis diagrams and the concept of shared electron pairs give a simple and common approach to covalent bonding in molecules,[3] but currently there is no such analogue for intermetallic phases. For electron rich molecules the consequence of shared (bonding) electron pairs, which are considered to form bonds between two atoms, is the formulation of free (non-bonding) electron pairs or so called lone pairs. At a further step chemists attribute a certain and three-dimensional space to these electron pairs and simple rules for the prediction of basic structures can be derived. The rules are summarized in the valence shell electron pair repulsion (VSEPR) concept.[4–6] Even we cannot imagine chemistry today without these heuristic concepts, the discussion becomes imprecise and diffuse when we look at these concepts on the basis of a quantum mechanical description. And the situation becomes even more difficult if we look at chemical bonding beyond the covalent case.[7,8]

The present article focuses on the description of the chemical bond on the basis of quantum chemistry and the interpretation of the results using the *Electron Localisation Function* (ELF) as introduced by Becke and Edgecombe.[9] This function focuses on the areas of localised electrons in molecules and solids rather than on metallic bonding. However, since there are also covalent contributions to metal–metal bonds, it is interesting to extract this information for metallic systems also.

In this article we show first the representation of chemical bonds and non-bonding electron pairs with the help of ELF for various molecules and ions with an emphasis on the relation to Lewis diagrams and the VSEPR model. Secondly, chemical bonding in so-called Zintl phases, *i.e.* extended solids where atoms fulfil the valence rules, will be analysed using tight binding methods.[10] Thirdly, ELF is used to analyse chemical bonding in metallic solids (intermetallic compounds).

2 The electron localisation function

In recent years some novel quantum mechanical tools have been derived to close the gap between useful, but heuristic concepts of chemical bonding and quantum theory. Especially theories based on the measurable electron density rather than on an orbital picture have been developed to justify chemists' intuitive view of bonding and non-bonding electron pairs and their three-dimensional shape or in other words the spatial localisation of electrons.[11,12] The ELF, that was originally introduced for the

 DOI: 10.1039/b202415m

deduction of the shell structure of atoms from the electron density,[9] allows the topographical analysis of the electron density distribution of molecules and as a consequence the partition of the molecular space into areas of high electron localisation. We know that due to the Pauli principle two electrons of same spin cannot occupy the same orbital. Thus the probability of finding another (test) electron of same spin (pair probability) in the vicinity of the electron of a hydrogen atom (the electron density might be approximated by the square of the 1s orbital) is 0. The electron density of a molecule can be approximated by the sum of the density of filled orbitals and the pair probability takes on values between 0 and ∞. The pair probability is low at those spatial regions where same spin electrons 'avoid' each other. In a chemical picture electrons are localised if they avoid each other. In consequence a region of low pair probability can be interpreted as an area of localized electrons. Since two electron pairs always contain two same spin electrons the same idea of electron localisation holds also for electron pairs.[13] In order to get a good representation the values of the pair probability between 0 and ∞ are normalized to the case of a homogenous electron gas and scaled in an inverse sense to values between 1 and 0. High ELF values and local ELF maxima correspond to areas and centres, respectively, of localised electrons and low ELF values are used to define the spatial area around these maxima. ELF can also be determined by the electron density alone in special view of the consideration of the Pauli principle.[14] Since the mathematical background of ELF has been subject of various articles,[15] we focus here on the graphical representation of ELF and its chemical interpretation.[13,16,17]

Let us consider the electron density distribution of an atom, which can be represented by the density of points as shown in Fig. 1a. Using a colour code for the values of ELF as shown in the colour bar at the bottom of Fig. 1d, ELF can be superimposed on the electron density by colouring each point of the electron density distribution in Fig. 1a. As result, we find radial localisation regions (Fig. 1b), which can be attributed to the shell structure of atoms, which is certainly not visible in Fig. 1a. For the three dimensional (3D) representation of spatial areas of localised electrons an isosurface (function at constant ELF value) is plotted. Generally the ELF value for isosurfaces are selected in such way, that areas around ELF maxima appear as distinct 3D regions (*e.g.* Fig. 1h–1j).

3 Bonding and non-bonding electron pairs in molecules and ions

As Lewis formulae split up the number of valence electrons in pairs of two, ELF divides a given electron density into different spatial regions. These areas correspond to the regions of localised chemical bonds. The case of the ethane molecule is shown in Figs. 1c and 1d. The uniform electron density distribution in Fig. 1c becomes structured by colouring it with ELF (Fig. 1d). Core electrons appear as white areas at the

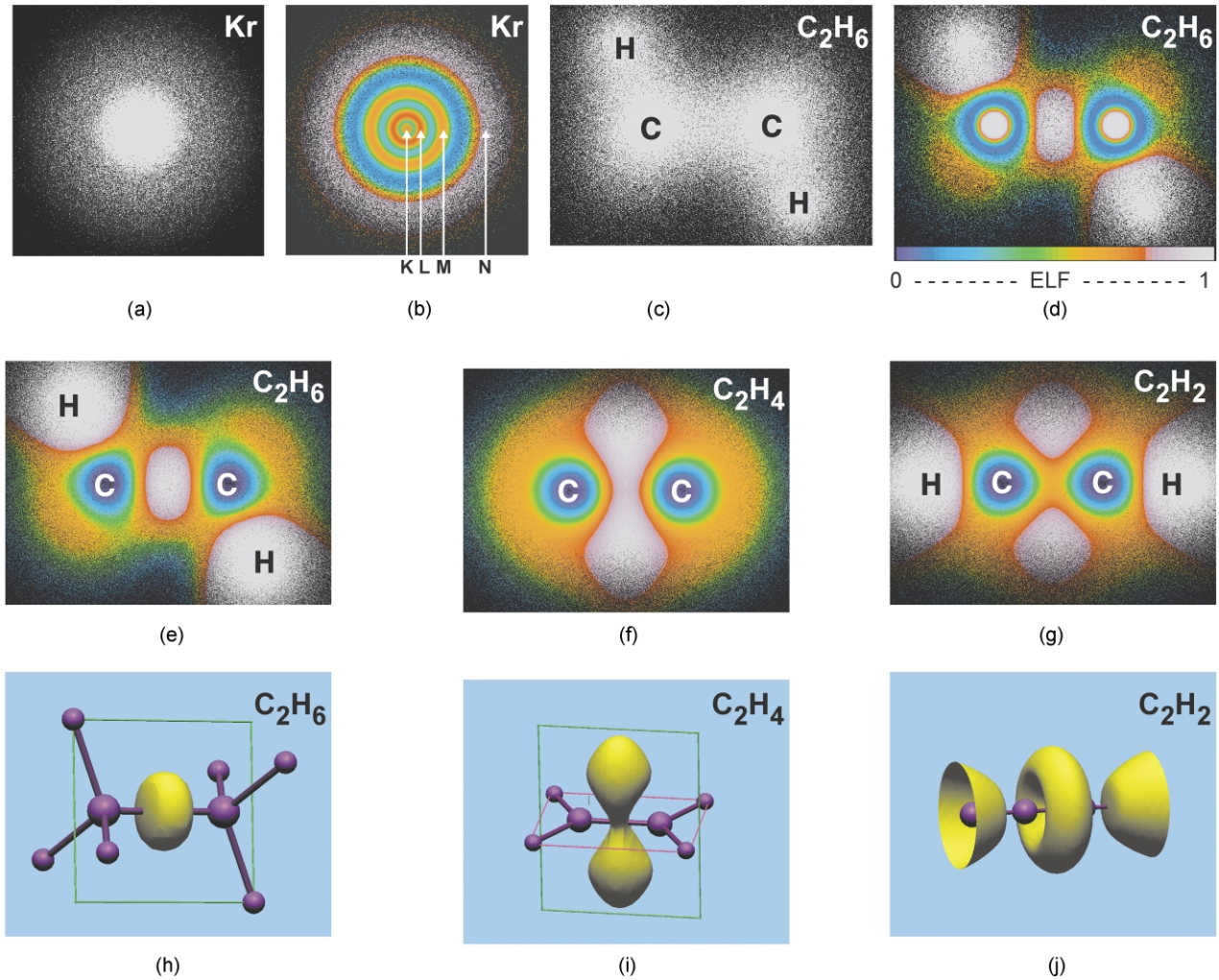

Fig. 1 (a) 2D-electron density distribution of Kr atom. (b) Colouring of the electron density distribution of a Kr atom with the values of ELF (colour bar see Fig. 1d). (c) Full electron 2D-electron density distribution of an ethane molecule. (d) Colouring of the electron density distribution in Fig. 1c with the values of ELF (colour bar see bottom). (e)–(g) 2D-valence electron density distribution with ELF colouring of a section through ethane, ethene, and ethine, respectively. (h)– (j) 3D-isosurface of ELF with ELF = 0.80 for the valence electron density of ethane, ethene, and ethyne, respectively.

position of the C atoms. The white area between the carbon atoms corresponds to a C–C single bond. In the case of the staggered ethane molecule two further white areas can be assigned to the two C–H bonds, which lie in the plane shown in Fig. 1d. The shapes of the areas, which correspond to the C–C and C–H bonds, are rather similar if only valence electrons are included for the calculation (Fig. 1e). In Fig. 1h the corresponding isosurface with ELF = 0.80 shows the area of the C–C bond; C–H bonds are omitted for reasons of clarity. Whereas a local ELF maximum on the atom–atom vector characterises a single bond, multiple bonds have maxima outside the connecting vector. There are two maxima—above and below the molecular plane—in ethene. The regions around these maxima are not separated for ELF = 0.80, but two distinct regions appear at higher ELF values (Figs. 1f and 1i). In ethyne there are not three maxima as might be expected for a triple bond, but the ELF maximum of the C≡C bond forms a ring between the two C atoms and perpendicular to the direction of the C–C bond vector (Figs. 1g and 1j). For ELF = 0.80 the isosurface has the shape of a torus. Since ELF is a property of the electron density and thus an observable (in the sense of quantum chemistry), the shape of the ELF region has to adapt the point symmetry of the molecule $D_{\infty h}$. In summary a single bond is characterised by a single ELF maximum on the atom–atom bond vector and multiple bonds by ELF maxima, which are located between two atoms but not on the atom–atom bond vector. In molecules with metal–metal quadruple bonds and D_{4h} symmetry such as $[Mo_2Cl_8]^{4-}$, ELF establishes the multiple-bond type by four distinct maxima between the metal atoms.[13]

A two dimensional image of NF_3 intersecting one N–F bond is shown in Fig. 2a. We recognize the unsymmetrical, polar bond ① between the atoms N and F as a separate region. The white area ② above the N atoms represents the lone pair located at the N atom. For ELF = 0.80 the lone pair regions around N and F atoms are clearly separated from each other and from the N–F bonding region, but the three lone pairs at the F atom appear as a single domain, *e.g.* due to the symmetry of the molecule the three lone pairs of the F atoms are not separated in three two-electron domains. Replacing N by P shows that the lone pair region located now at the P atom is larger and reflects the situation of the more diffuse character of the P-atom orbitals in a molecular orbital approach (Fig. 2c). In this case the P–F bonding region is not separated from the F atom lone pair domain. The situation of ClF_3 reflects nicely one of the VSEPR rules, which is that lone pairs occupy more space than bonding electron pairs. In other words: the repulsion between the two lone pairs ① and ② is stronger than between lone pairs and bonding electron pairs or between two bonding electron pairs. We find two maxima of ELF in the lone pair region of the central Cl atom. The basins ① and ② around the lone pair maxima are not totally separated for ELF = 0.80 (Fig. 2d), but appear as distinct regions at higher ELF values. Considering the VSEPR model, we say that the angle between the two lone pairs and the central atom is expected to be larger than 120° (five electron pairs and a pseudo trigonal-bipyramidal structure). We find that the ELF maxima of the lone pairs form an angle with central atom of ~160°. Notice, that the shape of the lone-pair region is simply a result of the T-type structure of the ClF_3 molecule. In the case of the linear $D_{\infty h}$ ClF_2^- we expect three lone pairs at the central Cl atom (Fig. 2e). The related ELF region has again the shape of a torus. The comparison with Fig. 1j shows that the shape of three lone pairs and three bonding electron pairs in linear molecules are rather similar.

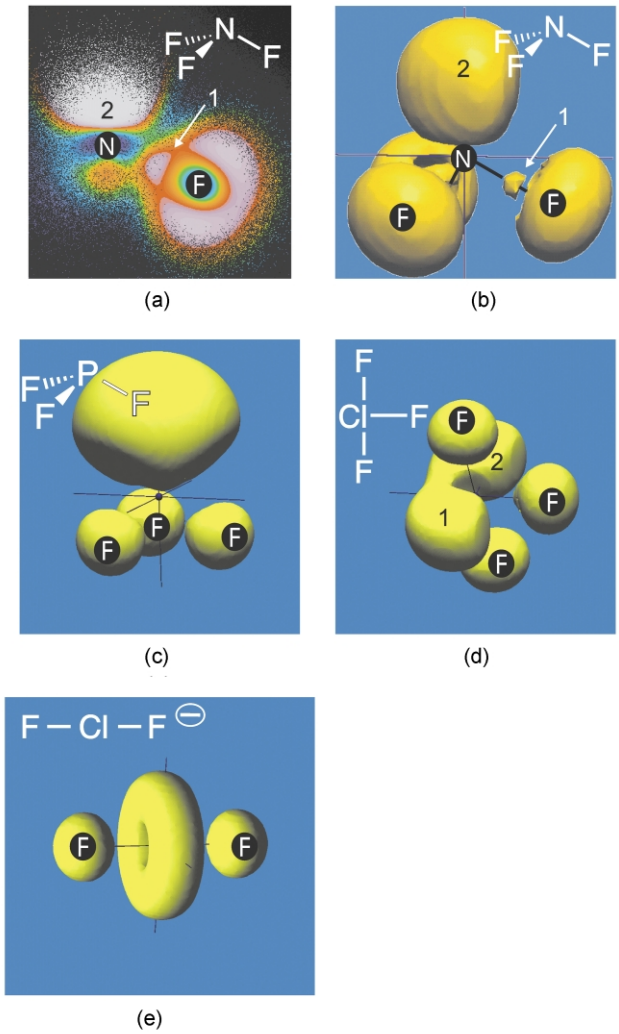

Fig. 2 (a) 2D-valence electron density distribution with ELF colouring of a section through NF_3.① and ② designate a polar N–F bond and the non-bonding electron pair at the N atom, respectively. (b)–(e) 3D-isosurface of ELF with ELF = 0.80 for the valence electron density of NF_3, PF_3, ClF_3, and ClF_2^-, respectively.

4 Lone pairs in the Zintl phases KSi, $K_6Sn_{23}Bi_2$ andK_6Sn_{25}

We will now investigate some solid-state compounds, in which all atoms fulfil the valence rules. According to the concept of Zintl, Klemm, and Busmann (ZKB) we can derive the structure of many polar intermetallic compounds. The structure of phases which are formed by an electropositive metal and a semi-metal of Group 13 to 15 (Zintl phases) can be rationalized by formal transfer of the valence electrons from the electropositive metal to the more electronegative component and applying valence concepts for the resulting anionic structure part as for molecules (8-N rule). In the binary phase NaSi we treat the resulting Si^{1-} anion with five valence electrons as a pseudo element of Group 15 and we find in analogy to the structure of white phosphorus the tetrahedral $[Si_4]^{4-}$ unit as building block in NaSi. The ELF of an isolated unit $[Si_4]^{4-}$ is shown in Fig. 3a.[13] There are six maxima outside the tetrahedron and located above the six edges, which represent two-electron-two-centre (2e-2c) bonds. The maxima are not on the Si–Si bond vectors and express the ring strain in the three-membered rings of the tetrahedron. Four larger regions represent the lone pairs located at each Si atom. The ELF can be derived in a similar way for extended solids using band structure calculations. The result of such a calculation for the solid NaSi or Na_4Si_4 is shown in Fig. 3b as yellow surface. For comparison the ELF regions of the isolated $[Si_4]^{4-}$ unit of Fig. 3a is superimposed as grid lines. Obviously the bond characteristics are the same, but the localisation domains are more contracted in the solid as compared to the case of isolated ions in the gas phase.

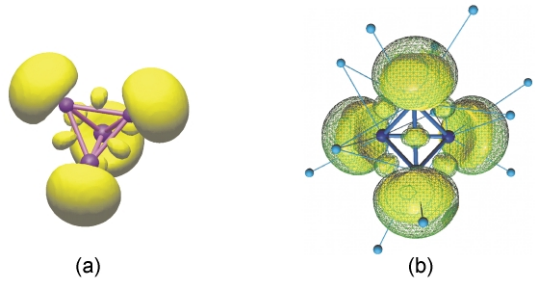

Fig. 3 (a) 3D-isosurface of ELF with ELF = 0.80 for the valence electron density of an isolated Si_4^{4-} unit. (b) As in Fig. 3a, but ELF is represented from a band structure calculation of the solid NaSi. For reasons of comparison the isosurface of Fig. 3a is represented in Fig. 3b as grid lines.

$K_6Sn_{23}Bi_2$ and K_6Sn_{25} crystallize in a rather interesting chiral clathrate-type structure and are built up from face sharing pentagon dodecahedral $Sn_{17}Bi_3$ and Sn_{20} units, respectively (Fig. 4a).[18] The pentagon dodecahedron is centred with a K atom and is connected to four others through three common faces and one external bond (Fig. 4b). The 3D network can also be constructed from penetrating helices, which consist of face sharing pentagon dodecahedra (Fig. 4c). Electropositive atoms occupy the resulting voids and channels. The connectivity of the 20 atoms of the pentagonal dodecahedra prompts the formulation: $[3b–E]_4[4b–E][4b–E]_{3\times 5/2}$ (3b and 4b are three- and four-bonded atoms, respectively) or with respect to the unit of 25 atoms: $[3b–E]_8[4b–E]_2[4b–E]_{15}$. In the case of exclusively Sn as E atoms the formula $[(3b–Sn)^-]_8[(4b–Sn)^0]_{17}$ or $[Sn_{25}]^{8-}$ and partial substitution of Sn atoms by Bi $[(3b–Sn)^-]_6[(3b–Bi)^0]_2[(4b–E)^0]_{17}$ or $[Sn_{23}Bi_2]^{6-}$ results for the anionic structure part. According to the 8-N rule $K_6Sn_{23}Bi_2$ is electron precise and K_6Sn_{25} has an electron deficiency of two electrons per formula unit.

One of the remarkable features of the Extended Hückel band structure and density of states (DOS) of a rigid band model $K_6Sn_{25}^{2-}$ (*e.g.* the calculation is carried out for the composition K_6Sn_{25} but with the electron number of $K_6Sn_{23}Bi_2$) is a large band gap of several eVs indicative of a Zintl phase (Fig. 5a). The band structure and DOS are shown from the lower energy region up to the Fermi level, antibonding states are located several eV above E_F. All bands are rather flat implying a high covalent character of the chemical bond. The ELF in Fig. 5b

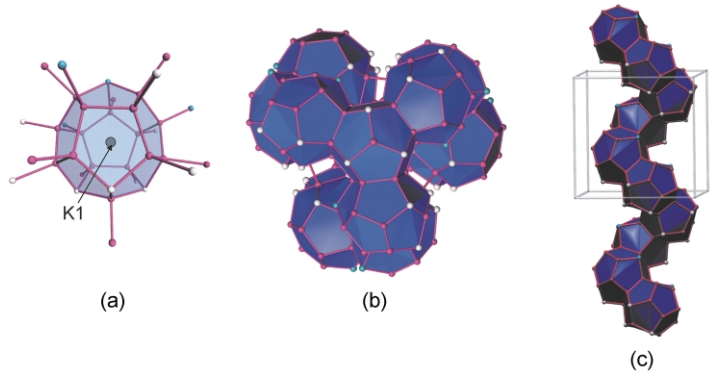

Fig. 4 (a)–(c) Structure details of $K_6Sn_{23}Bi_2$: (a) one type of pentagon dodecahedron as building block; (b) structure detail with face sharing pentagon dodecahedra and external bonds; (c) a helix of pentagon dodecahedra.

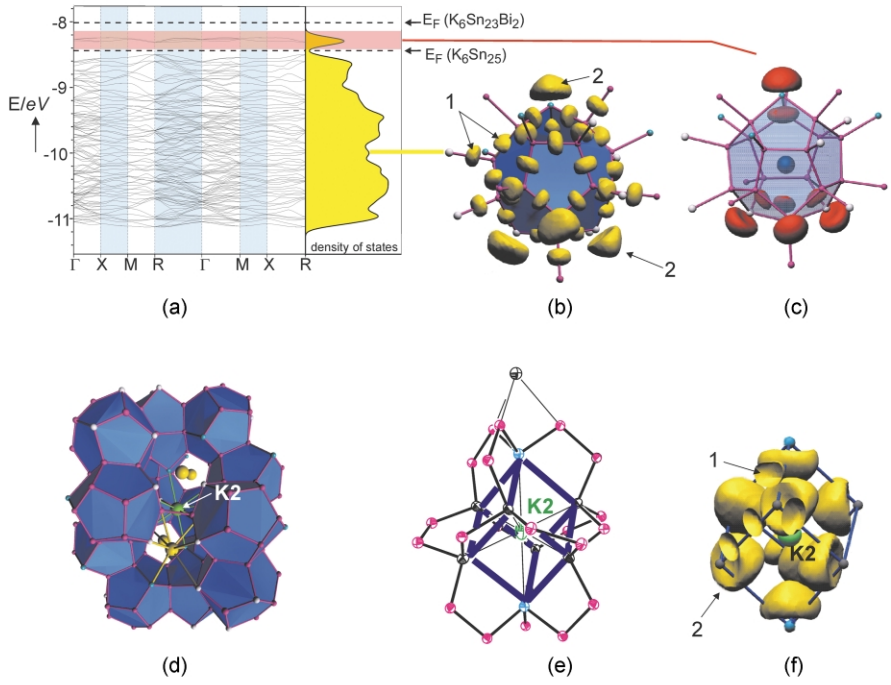

Fig. 5 (a) Band structure and density of states on the basis of an Extended Hückel calculation of a rigid band model of $K_6Sn_{25}^{2-}$. The Yellow area corresponds to filled states up to the Fermi level E_F. (b) 3D-isosurface of ELF with ELF = 0.80 of one pentagon dodecahedron. ① and ② designate bonding and non-bonding electron pairs, respectively. (c) The partial electron density of the top most bands in the vicinity of a pentagon dodecahedron in $K_6Sn_{23}Bi_2$. The top most bands are shaded in red in Fig. 5a. (d) Structure detail of $K_6Sn_{23}Bi_2$ including the eight pentagon dodecahedra around the K2 atom. (e) 3b atoms of eight pentagon dodecahedra, which form a distorted cube around K2; additional atoms are part of the adjacent pentagon dodecahedra. (f) 3D-isosurface of ELF with ELF = 0.80 in the vicinity of K2. ① and ② designate bonding and non-bonding electron pairs, respectively.

shows that all contacts of the anionic framework correspond to localised 2e-2c bonds and that the 3b atoms possess one lone pair each.[19] Lone pairs similar to sp^3-type hybrid orbitals in molecules but as a result from band structure calculations can alternatively be visualized using partial electron density (PED) representations as shown in Fig. 5c.[20] An isosurface of the electron density calculated from the flat bands at E_F within the energy region indicated by the red background in Fig. 5a, adopts the shape of four sp^3-orbital type areas. We see that in this solid lone pair states are located at the Fermi level, which can be seen in similarity to molecules where lone pairs are the highest occupied orbitals (HOMO).

A second and small band gap just below the Fermi level corresponding to the electron count of $K_6Sn_{25}^{2-}$ or $K_6Sn_{23}Bi_2$ explains the stability of the electron deficient phase K_6Sn_{25}. There is one band (holding two electrons) per formula unit pushed to higher energy. As pointed out already, the real space representation of the electron density of this band section (PED) shows that s-p mixing occurs along all symmetry lines in reciprocal space forming four sp^3-type crystal orbital hybrids, which point to the outside of each pentagon dodecahedron (Fig. 5c). The destabilisation of the bands close to the Fermi level arises from interactions between non-bonding electron pairs of the 3b atoms around the position of K2. There are eight lone pairs located at the corners inside of a distorted cubic cavity of three-connected framework atoms. Each vertex of the cube belongs to one pentagon dodecahedron (Figs. 5d and 5e) and the lone pairs point towards the central K2 atom. The closeness of the eight lone pairs inside this cube (Fig. 5f) leads to the destabilisation of one of the eight resulting bands (crystal orbitals). Instead of the more common four-electron-two-centre repulsive interaction we find in this case a 16-electron-8-centre repulsive interaction. Thus, K_6Sn_{25} can be described as a Zintl phase with a two-electron deficiency due to the interaction of the lone pairs.

5 At the border to intermetallic compounds: $NaSn_5$

$NaSn_5$ represents an example of a tin network with alternate tetravalent atoms (black Sn1 and Sn2 atoms in Fig. 6a) and tin atoms with coordination number five (green Sn3 atoms). The 4b atoms form a 2D net of exclusively five-membered rings, which is connected to the slightly corrugated quadratic net of the five-bonded (5b) atoms. The atom–atom separations between 4b atoms are close to the value of 2.81 Å in α-Sn, in which all Sn–Sn contacts correspond to localised 2e-2c bonds. The structure detail in Fig. 6b shows that five-membered rings of 4b atoms form a fragment of a pentagon dodecahedron around each Na position. This polyhedral fragment of twelve 4b atoms spans eight Sn3 atoms of the quadratic net and is thus topologically related to a pentagon dodecahedron of twenty (12 + 8 = 20) tin atoms. The two-dimensional connectivity of the pentagon dodecahedral fragments leads to a slab of four-coordinate atoms that stack, alternating with the quadratic network of five-coordinated atoms, along the z direction. The Sn–Sn separation of 5b atoms (Fig. 6a) are in the range of the values of the metallic β-Sn modification (3.02 and 3.18 Å).[21]

Band structure and DOS calculations predict that $NaSn_5$ is an anisotropic conductor (Fig. 6c). The density of states at the Fermi level E_F can be traced to predominant contributions of Sn3 atoms and steep bands crossing the Fermi level are almost completely Sn3-p_x and -p_y orbital in character, *i.e.* metallic conductivity propagates predominantly over states with Sn3 orbital contributions.

For $NaSn_5$ one can clearly recognise regions ① with ELF > 0.8 between the atom Sn1 and Sn2, which are characteristic for 2e-2c bonds (Fig. 6b). The ELF region ② between the Sn2 and Sn3 atoms is not symmetric with respect to the two atoms and typical of a polar bond. Notice the rather similar shape of the polar N–F bond in Fig. 2a and 2b. In $NaSn_5$ the ELF shows no local maximum on the nucleus–nucleus bonding lines between Sn3 atoms, however at the Sn3 atoms regions of lone pairs ③ are apparent, which are directed toward the electropositive Na atom. In $NaSn_5$ ELF enables the structure parts with localised and delocalised bonds to be distinguished. Interestingly, localised electron domains occur also at those atoms, which belong to the 'metallic' part of the structure. The shape of these localised-electron regions can be interpreted as if they are lone pairs located at the atoms of the 'metallic' substructure.

6 The role of lone pairs in superconducting $BaSn_3$ and $BaSn_5$

$BaSn_3$ is built up by linear chains of face sharing Sn_6 octahedra, which are separated by Ba atoms (Fig. 7a). The distortion of the atoms in $BaSn_3$ from an ideal hexagonal closed packed array leads to shorter Sn–Sn contacts within the hexagonal layers compared to the interlayer contacts. If we consider only the shortest Sn–Sn contact, a triangular Sn_3 unit appears as building block. Using the ZKB concept we could deduce the formula Sn_3^{2-}, a formula that has—considering a 2π-electron aromatic system—the same number of valence electrons as the cyclopropenyl cation $C_3R_3^+$.[22]

The band structure of $BaSn_3$ (Fig. 7c) features a large dispersion of bands along the symmetry lines parallel to the chain direction (Γ-A). Bands along symmetry points parallel to the layers are comparatively flat (*e.g.* μ-Γ, A-L-H-A). Again an anisotropic metallic conductivity is apparent in $BaSn_3$ with the special situation that bands near E_F run flat through the zone centre Γ. As can be seen from the analysis of the individual bands (so-called fat band analysis) this narrow band region energetically close to E_F originates from contributions of p-orbitals within the plane of the Sn3 unit (p_x and p_y) and of s

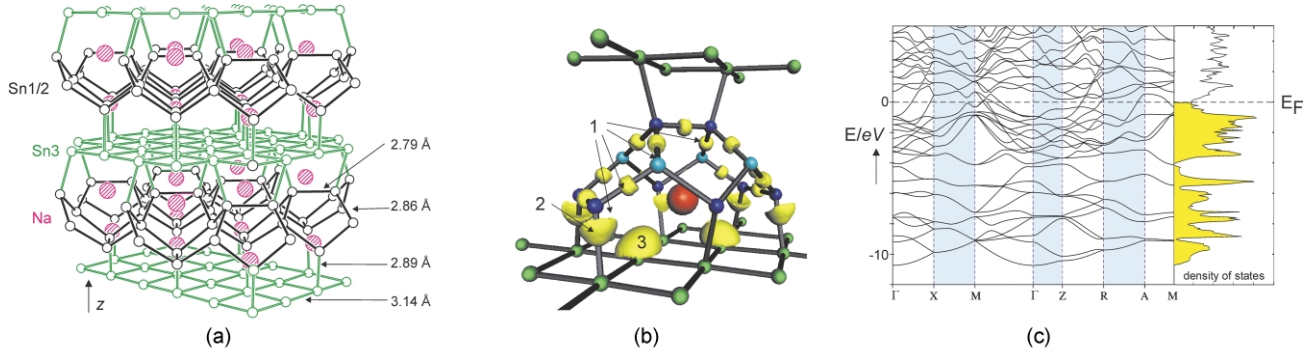

Fig. 6 (a) Structure detail of $NaSn_5$. (b) Structure detail of $NaSn_5$ with 3D-isosurface of ELF = 0.80. ①, ②, and ③ designate bonding electron pairs, polar bonds, and non-bonding electron pairs, respectively. (c) LMTO (linear muffin tin orbital)-band structure and density of states on the basis of density functional theory for $NaSn_5$. Yellow area corresponds to filled states up to the Fermi level E_F.

orbitals. Orbital mixing leads to the formation of sp^2-type lone pairs at Sn atoms. The lone pairs become visible by ELF representations (Figs. 7a and 7b). Three outer ELF areas with half-moon shapes ② correspond to the lone pairs at the tin atoms, three smaller regions ①, at lower ELF values and which are better visible in the two-dimensional representation in Fig. 7b, can be attributed to the Sn–Sn bonds of the triangular units. The lone pairs ② are flattened, owing to interactions with lone pairs of neighbouring units. The interaction of the lone pairs between the strings of Sn atoms is responsible for a certain dispersion of the flats bands at E_F and for the elevation of this bands above E_F.[22] Interactions of the 2π-electrons of the Sn_3^{2-} building blocks stacking along the z direction leads to the steep bands crossing E_F.

$BaSn_5$ can be derived from the AlB_2 structure type. Pairs of graphite-like layers of Sn atoms (Sn1) form hexagonal prisms. Each prism is centred by another tin atom (Sn2), which in consequence has the coordination number 12. 6^3 nets of Ba atoms with Ba above the centre of each tin hexagon (Fig. 8a) separate the two-dimensional tin slabs which can also be described two 3^6 nets of Sn1 and one 6^3 net of Sn2 atoms.[23]

Band structure and density of states plots (Fig. 8c) reveal the metallic property of $BaSn_5$. The Fermi level E_F cuts the DOS at a flank of a local DOS maximum. The band structure plot features bands with large dispersions crossing E_F (*e.g.* Γ-A) and band sequences crossing the zone centre Γ at E_F with little dispersion. Thus the situation resembles the one of $BaSn_3$. The narrow band region is most distinct around the saddle point along the symmetry path M–Γ close to Γ. As can be seen from a fat band analysis the flat portion of the bands originates in the vicinity of E_F and around Γ mainly from the Sn1-p orbitals.

The image in Fig. 8b shows a three-dimensional isosurface of ELF, which indicates the presence of lone pairs ② at Sn1, which are located above and below the hexagonal prisms, two lone pair regions ③ at the centring Sn2 atoms and region of localised bonds ① between two Sn1 atoms. The combined information of the band characteristics at E_F and the ELF analysis shows that lone pairs are energetically located at E_F and that they are directed perpendicular to the hexagonal layers towards the lone pairs of adjacent layers.

The importance of saddle points in the band structure and the associated van Hove singularities in the DOS (local maximum)[21] is generally applied for the cuprate superconductors.[24,25] The inspection of the band structures in Figs. 7c and 8c shows that the concept of the van Hove scenario can also be discussed for intermetallic superconductors and the following qualitative picture of the electron–phonon interactions can be deduced:[22,23,26] A point of inflection near Γ gives rise to a local maximum in the electronic DOS at E_F. Real space analysis of the electronic structure with the help of ELF reveals that non-bonding electron pairs are associated with the DOS maximum at E_F. Lattice vibrations will change the interaction of the lone pairs of two adjacent atom chains ($BaSn_3$) or layers ($BaSn_5$) and thus influence the energy of the corresponding narrow bands of paired electrons. Repulsive interaction between the lone pairs will raise the energy of the filled band. If the lone pairs are located close enough at E_F, repulsive interaction will shift them above E_F and electrons, which populate these localised states (flat bands), will subsequently be transferred to 'metallic' bands (disperse bands crossing E_F), which now lie lower in energy. Thus transitions between localised (narrow bands) and delocalised electrons (bands of high dispersion) can occur in dependency of lattice vibrations (and *vice versa*). Recently, the relation of the occurrence of localised electrons in the form of lone pairs in intermetallic compounds and superconductivity was also pointed out for the superconductors K_5Pb_{24}[27] and $SrSn_3$.[26] The ideas are also closely related to the mechanism of local electron pairing in π* bands of rare earth metal carbide halides.[28]

7 Discussion

ELF pictorially describes chemists' intuitive ideas of single and multiple bonds as well as non-bonding electron pairs. Classical concepts such as the Lewis formula, VSEPR and ZKB are corroborated and ELF enables the transfer of the picture of the chemical bond in molecules to intermetallic compounds in a unique way.

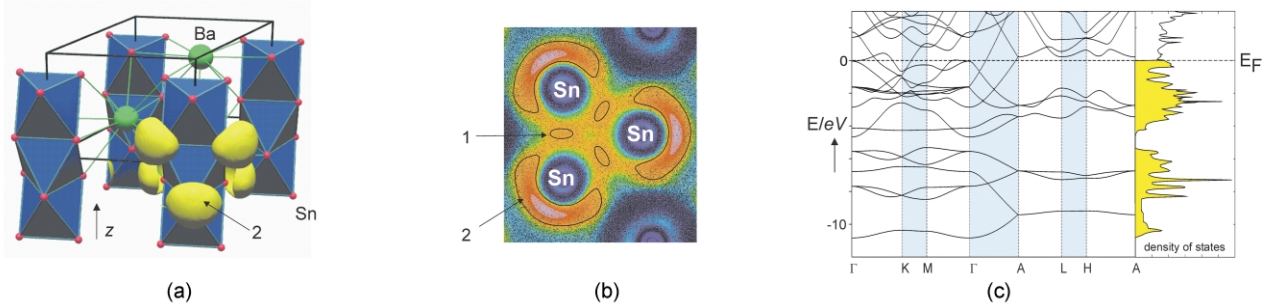

Fig. 7 (a) Structure detail and 3D-isosurface of ELF with ELF = 0.75 of $BaSn_3$. (b) 2D-LMTO-valence electron density distribution with ELF colouring of a section through three adjacent Sn atoms perpendicular to the z direction (colour bar see Fig. 1d). ① and ② designate bonding and non-bonding electron pairs, respectively. The lines correspond to ELF = 0.65. (c) LMTO-band structure and density of states on the basis of density functional theory for $BaSn_3$. Yellow area corresponds to filled states up to the Fermi level E_F.

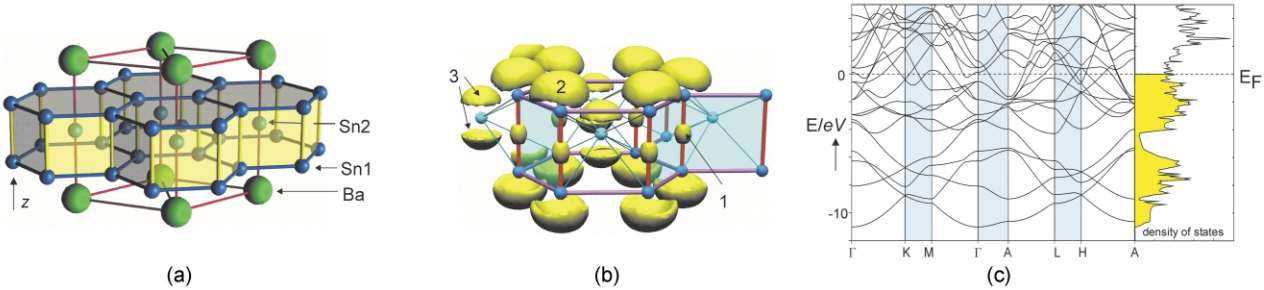

Fig. 8 (a) Structure detail of $BaSn_5$. (b) Structure detail of $BaSn_5$ with 3D-isosurface of ELF with ELF = 0.77. ① designates the localised Sn–Sn bond, ② and ③ non-bonding electron pair domains at Sn1 and Sn2, respectively. (c) LMTO-band structure and density of states on the basis of density functional theory for $BaSn_5$. Yellow area corresponds to filled states up to the Fermi level E_F.

In intermetallic compounds localised chemical bonds appear in the form of bonding and non-bonding electron pair domains. As in molecules where non-bonding electron pairs are often energetically located at the top most energy levels (HOMO), non-bonding electron pairs are located energetically close to the Fermi level in polar intermetallic compounds. As in molecules non-bonding electron pairs affect the chemical reactivity (Lewis base) and non-bonding interactions influence the structure of molecules,[29] non-bonding electron pairs in intermetallic compounds have an influence on the electronic properties.

The mechanism of local electron pair formation[30] brought up ideas of a *chemical view* of superconductivity, which is given through inspection of the band structure for the coincident appearance of quasi-molecular states (localisation) and disperse bands crossing the Fermi level (delocalisation).[25,31,32] Local electron pair formation takes place in metals with narrow band regions and such narrow band regions originate in polar intermetallic compounds from lone pairs, which are located at the atoms of the more electronegative component. As a consequence further superconductors might be expected in metallic Zintl phases.

8 Summary

1. Lone pairs are present in many Zintl phases as expected by the 8-N rule.

2. Lone pairs in solids are generally more contracted than in isolated units. This originates from the repulsive interactions between electron pairs.

3. In polar intermetallic compounds characteristics of localised bonds occur mainly as lone pairs. The lone pairs are predominantly located in empty cavities, or cavities which are occupied by the more electropositive atoms.

4. Lone pairs in intermetallic compounds are correlated to flat band sections in the electronic band structure. Lone pair repulsion is associated with increased band dispersion or destabilisation of the corresponding bands.

5. A change in magnitude of repulsive lone pair interactions (as due to lattice vibrations) can lead to a band shift of narrow bands (localised electrons) above the Fermi level resulting in an electron transfer from localised to delocalised bands and *vice versa*. This mechanism of local electron pair formation gives rise to ideas of a *chemical view* of the phenomenon of superconductivity in intermetallic compounds.

9 Acknowledgment

The author would like to thank Dr M. Schreyer for looking through the manuscript.

References

1 L. Pauling, in *The Chemical Bond—Structure and Dynamics*, ed. A. Zewail, Boston, 1992.
2 C. Belin and M. Tillard-Charbonnel, *Coord. Chem. Rev.*, 1998, **178–180**, 529.
3 G. H. Purser, *J. Chem. Educ.*, 1999, **76**, 1013.
4 R. Gillespie and R. S. Nyholm, *Quart. Rev. Chem. Soc.*, 1957, **11**, 339.
5 I. Hargittai, *Coord. Chem. Rev.*, 2000, **197**, 21.
6 R. J. Gillespie and E. A. Robinson, *Angew. Chem., Int. Ed. Engl.*, 1996, **35**, 495.
7 See correspondenz between L. C. Allen, J. K. Burdett and J. C. Schön, *Angew. Chem., Int. Ed. Engl.*, 1995, **34**, 2003.
8 J. J. Gilman, *J. Chem. Educ.*, 1999, **76**, 1330.
9 A. D. Becke and E. Edgecombe, *J. Chem. Phys.*, 1990, **92**, 5397.
10 R. Hoffmann, *Solids and Surfaces. A Chemist's View of Bonding an Extended Surfaces*, VCH Verlagsgesellschaft, 1988.
11 R. F. W. Bader, *Atoms in Molecules—A Quantum Theory*, Oxford University Press, 1990.
12 R. F. W. Bader, *Coord. Chem. Rev.*, 2000, **197**, 71.
13 T. F. Fässler and A. Savin, *Chem. Unserer Zeit.*, 1997, **31**, 110.
14 M. Kohout and A. Savin, *J. Comp. Chem.*, 1997, **18**, 1431.
15 ELF is based on the Hartree–Fock pair probability of parallel spin electrons and is thus a measure of the Pauli repulsion[9] or is calculated in density functional theory from the excess kinetic energy density due to Pauli repulsion.[33] Since both methods use solely $\nabla\rho$ and $\nabla\varphi$ (ρ electron density, φ orbitals) to derive ELF, this function can also be calculated by other methods such as the Extended Hückel method. ELF is scaled to values between 0 and 1 with the meaning that ELF values close to one correspond to highly localised electrons as it is typically found for 2e-2c bonds or non-bonding electron pairs in molecules. In polar intermetallic compounds ELF has generally smaller values than in valence compounds, but ELF maxima still count for centres of localised chemical bonds.[16,34,35] ELF images in Figs. 1a–1d were calculated on Hartree–Fock level; 1e–j, 2a–e, 3a, 3b, 5b, and 5f on Extended Hückel level, and in Figs. 6, 7 and 8 using density functional theory (LMTO-ASA: linear muffin tin orbital with atomic sphere approximation). For an overview of the ELF see also: http://www.cpfs.mpg.de/ELF.
16 A. Savin, A. D. Becke, J. Flad, R. Nesper and H. G. von Schnering, *Angew. Chem., Int. Ed. Engl.*, 1991, **31**, 185.
17 A. Savin, R. Nesper, S. Wengert and T. F. Fässler, *Angew. Chem., Int. Ed. Engl.*, 1997, **36**, 1808.
18 T. F. Fässler and C. Kronseder, *Z. Anorg. Allg. Chem.*, 1998, **624**, 561.
19 T. F. Fässler, *Z. Anorg. Allg. Chem.*, 1998, **624**, 569.
20 T. F. Fässler, U. Häußermann and R. Nesper, *Chem. Eur. J.*, 1995, **1**, 625.
21 T. F. Fässler and C. Kronseder, *Angew. Chem., Int. Ed.*, 1998, **37**, 1571.
22 T. F. Fässler and C. Kronseder, *Angew. Chem., Int. Ed. Engl.*, 1997, **36**, 2683.
23 T. F. Fässler, S. Hoffmann and C. Kronseder, *Z. Anorg. Allg. Chem.*, 2001, **620**, 2486.
24 D. M. Newns, H. R. Krishnamurthy, P. C. Pattnaik, C. C. Tsuei, C. C. Chi and C. L. Kane, *Physica B*, 1993, **186–188**, 801.
25 A. Simon, *Angew. Chem., Int. Ed. Engl.*, 1997, **36**, 1788.
26 T. F. Fässler and S. Hoffmann, *Z. Anorg. Allg. Chem.*, 2000, **620**, 106.
27 T. F. Fässler, C. Kronseder and M. Wörle, *Z. Anorg. Allg. Chem.*, 1999, **625**, 15.
28 A. Simon, A. Yoshiasa, M. Bäcker, R. W. Henn, C. Felser, R. K. Kremer and H. Mattausch, *Z. Anorg. Allg. Chem.*, 1996, **622**, 123.
29 L. S. Bartell, *J. Chem. Phys.*, 1960, **32**, 827.
30 R. Micnas, J. Ranninger and S. Robaszkiewicz, *Rev. Mod. Phys.*, 1990, **62**, 113.
31 A. Simon, *Angew. Chem., Int. Ed. Engl.*, 1987, **26**, 579.
32 A. Simon, *Chem. Unserer Zeit.*, 1988, **22**, 1.
33 A. Savin, H. J. Flad, J. Flad, H. Preuss and H. G. von Schnering, *Angew. Chem., Int. Ed. Engl.*, 1992, **31**, 185.
34 U. Häußermann, S. Wengert, P. Hofmann, A. Savin, O. Jepsen and R. Nesper, *Angew. Chem., Int. Ed. Engl.*, 1994, **33**, 2069.
35 U. Häußermann, S. Wengert and R. Nesper, *Angew. Chem., Int. Ed. Engl.*, 1994, **33**, 2073.